

# Controlled Syntheses of Aligned Multi-Walled Carbon Nanotubes: Catalyst Particle Size and Density Control via Layer-by-Layer Assembling

Jianwei Liu, Xiaojun Li, Amanda Schrand, Toshiyuki Ohashi,<sup>†</sup> and Liming Dai\*

Department of Chemical and Materials Engineering, School of Engineering, University of Dayton,  
300 College Park, Dayton, Ohio 45469-0240

Received July 12, 2005. Revised Manuscript Received October 24, 2005

Using the layer-by-layer assembly method, we have fabricated catalyst particles of a controlled size distribution and packing density for aligned carbon nanotube growth. In particular, poly(sodium-4-styrenesulfonate), PSS, and iron hydroxide colloid were layer-by-layer assembled via the electrostatic interaction onto an acetic-acid-plasma treated quartz plate. This multilayer catalyst precursor film was then calcined in Ar/H<sub>2</sub> at 750 °C to produce iron nanoparticles for the subsequent growth of carbon nanotubes at 750 °C under a combined flow of Ar/H<sub>2</sub> and C<sub>2</sub>H<sub>2</sub>. UV–vis absorption and X-ray photoelectron spectroscopic (XPS) measurements confirm the consecutive formation of the iron hydroxide colloid/PSS multilayer films. Atomic force and electron microscopic (AFM, SEM, TEM) imaging shows that the catalyst particles thus prepared possess a layer-number-dependent size distribution and packing density after calcination. Aligned multi-walled carbon nanotubes with a controlled structure and morphology were produced from judiciously designed layer-by-layer assembled multilayer catalyst precursor films with a desirable layer number and composition.

## Introduction

Since the discovery of carbon nanotubes by Iijima in 1991,<sup>1</sup> considerable efforts have been made to study their preparation, growth mechanism, and potential applications.<sup>2–5</sup> In particular, the aligned growth of carbon nanotubes has brought great promise for their potential applications in field-emitting flat panel displays and many other systems.<sup>6–9</sup> Although several postsynthesis fabrication techniques and synthesis-induced alignment methods have been devised to prepare aligned *multi-walled* carbon nanotubes (MWNTs),<sup>10–15</sup> the preparation of perpendicularly aligned *single-walled*

carbon nanotubes (SWNTs) is only a recent development.<sup>16,17</sup> To grow perpendicularly aligned SWNTs, it is necessary to have nanometer-sized catalyst particles densely packed on the substrate surface to promote strong van der Waals forces between the growing carbon nanotubes for facilitating the alignment.<sup>18–24</sup> One of the very delicate and vital issues to be addressed is, therefore, how to prepare densely packed catalyst nanoparticles while largely retaining their structural integrity without segregation, even at the elevated temperatures required for the aligned carbon nanotube growth.

On the other hand, the layer-by-layer (LBL) assembling process,<sup>25,26</sup> in which multilayer films are prepared by

\* To whom correspondence should be addressed. E-mail: ldai@udayton.edu.

<sup>†</sup> On leave of absence from Honda R&D Co., Ltd Wako Research Center 1-4-1 Chuo, Wako-shi, Saitama, 351-0193 Japan as a visiting scientist at UD.

- (1) Iijima, S. *Nature* **1991**, *354*, 56.
- (2) Harris, P. J. F. *Carbon Nanotubes and Related Structures—New Materials for the Twenty-First Century*; Cambridge University Press: Cambridge, U.K., 2001.
- (3) Saito, R.; Dresselhaus, G.; Dresselhaus, M. S. *Physical Properties of Carbon Nanotubes*; Imperial College Press: London, 1998.
- (4) Dai, L. *Intelligent Macromolecules for Smart Devices: From Materials Synthesis to Device Applications*; Springer-Verlag: London, 2004.
- (5) Baughman, R. H.; Zakhidov, A. A.; de Heer, W. A. *Science* **2002**, *297*, 787.
- (6) Schmid, H.; Fink, H. W. *Appl. Phys. Lett.* **1997**, *70*, 2679.
- (7) Rao, A. M.; Jacques, D.; Haddon, R. C.; Zhu, W.; Bower, C.; Jin, S. *Appl. Phys. Lett.* **2000**, *76*, 3813.
- (8) Tans, S. J.; Verschueren, A. R. M.; Dekker, C. *Nature* **1998**, *393*, 49.
- (9) Keren, K.; Berman, R. S.; Buchstab, E.; Sivan, U.; Braun, E. *Science* **2003**, *302*, 1380.
- (10) Dai, L.; Patil, A.; Gong, X.; Guo, Z.; Liu, L.; Liu, Y.; Zhu, D. *ChemPhysChem* **2003**, *4*, 1150, and references therein.
- (11) Li, W. Z.; Xie, S. S.; Qian, L. X.; Chang, B. H.; Zou, B. S.; Zhou, W. Y.; Zhao, R. A.; Wang, G. *Science* **1996**, *274*, 1701.
- (12) Fan, S.; Chapline, M. G.; Frank, N. R.; Tomblin, T. W.; Cassell, A. M.; Dai, H. *Science* **1999**, *283*, 512.
- (13) de Heer, W. A.; Bonard, J. M.; Fauth, K.; Chatelain, A.; Forro, L.; Ugarte, D. *Adv. Mater.* **1997**, *9*, 87.
- (14) Rao, C. N. R.; Sen, R.; Satishkumar, B. C.; Govindaraj, A. *Chem. Commun.* **1998**, 1525.
- (15) Ren, Z. F.; Huang, Z. P.; Xu, J. H.; Wang, P. B.; Siegal, M. P.; Provencio, P. N. *Science* **1998**, *282*, 1105.
- (16) Murakami, Y.; Chiashi, S.; Miyauchi, Y.; Hu, M.; Ogura, M.; Okubo, T.; Maruyama, S. *Chem. Phys. Lett.* **2004**, *385*, 298.
- (17) Hata, K.; Futaba, D. N.; Mizuno, K.; Namai, T.; Yumura, M.; Iijima, S. *Science* **2004**, *306*, 1362.
- (18) Huang, S.; Dai, L.; Mau, A. W. H. *J. Mater. Chem.* **1999**, *9*, 1221.
- (19) Huang, S.; Dai, L.; Mau, A. W. H. *J. Phys. Chem. B* **1999**, *103*, 4223.
- (20) Murakami, Y.; Chiashi, S.; Miyauchi, Y.; Hu, M. H.; Ogura, M.; Okubo, T.; Maruyama, S. *Chem. Phys. Lett.* **2004**, *385*, 298.
- (21) Terrones, M.; Grobert, N.; Olivares, J.; Zhang, J. P.; Terrones, H.; Kordatos, K.; Hsu, W. K.; Hare, J. P.; Townsend, P. D.; Prassides, K.; Cheetham, A. K.; Kroto, H. W.; Walton, D. R. M. *Nature* **1997**, *388*, 52.
- (22) Geoghegan, D. B.; Puzos, A. A.; Ivanov, I. N.; Jesse, S.; Eres, G.; Howe, J. Y. *Appl. Phys. Lett.* **2003**, *83*, 1851.
- (23) Wei, B. Q.; Vajtai, R.; Jung, Y.; Ward, J.; Zhang, R.; Ramanath, G.; Ajayan, P. M. *Nature* **2002**, *416*, 495.
- (24) Kim, N. S.; Lee, Y. T.; Park, J.; Han, J. B.; Choi, Y. S.; Choi, S. Y.; Choo, J.; Lee, G. H. *J. Phys. Chem. B* **2003**, *107*, 9249.
- (25) Singh, C.; Shaffer, M. S.; Windle, A. H. *Carbon* **2003**, *41*, 359.
- (26) Hammond, P. T. *Adv. Mater.* **2004**, *16*, 1271.
- (27) Hi, X. Y.; Shen, M. W.; Mohwald, H. *Prog. Polym. Sci.* **2004**, *29*, 987.

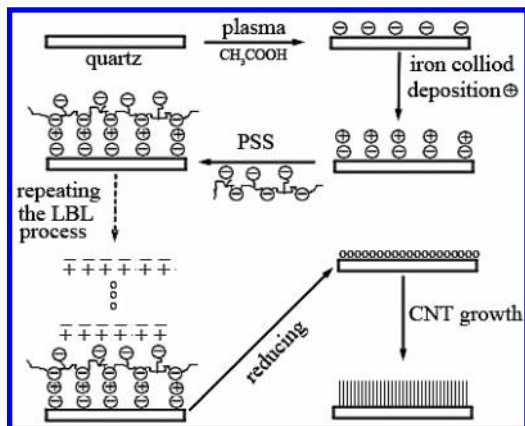


**Figure 1.** Schematic illustration of the procedures for the layer-by-layer assembling of the iron hydroxide colloidal nanoparticles and PSS, followed by the catalyst nanoparticle reduction (calcination) and growth of aligned carbon nanotubes.

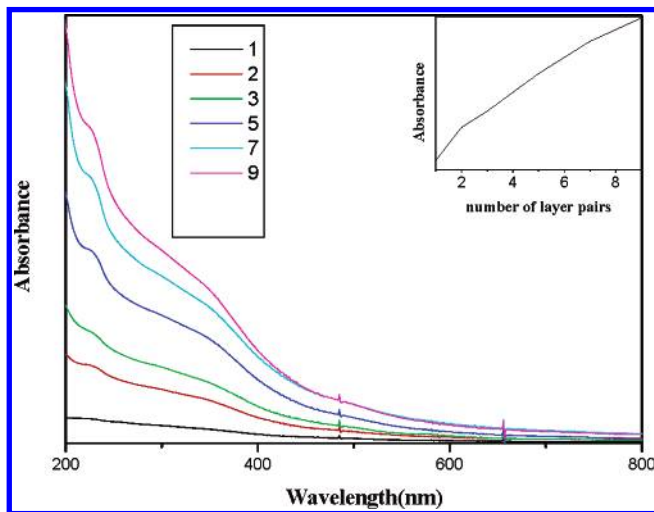


**Figure 2.** UV-vis absorption spectra for the PSS/iron hydroxide colloid layer pair deposited on a quartz substrate. The inset shows a plot of absorbance at 225 nm vs the number of layer pairs.

alternating adsorption of anionic and cationic bipolar components onto substrate surfaces via the electrostatic attraction between opposite charges, has been proven a powerful technique for fabricating various nanomaterials, including nanoparticle-intercalated multilayer polymer films.<sup>27–29</sup> In our further investigation on the growth of aligned carbon nanotubes, we have recently found that catalyst particles of a controlled size distribution and packing density can be prepared via the layer-by-layer assembling of poly(sodium-4-styrenesulfonate), PSS, and iron hydroxide colloid onto an acetic-acid-plasma treated quartz plate, followed by reducing with a combined flow of Ar/H<sub>2</sub> at 750 °C. In comparison with the simple casting of a reverse micelle solution of metal nanoparticles for aligned MWNT growth previously reported,<sup>30</sup> the layer-by-layer assembling method provides advantages for effectively controlling the resultant particle density by regulating the layer number. The particle size distribution can also be tuned by changing the relative amounts

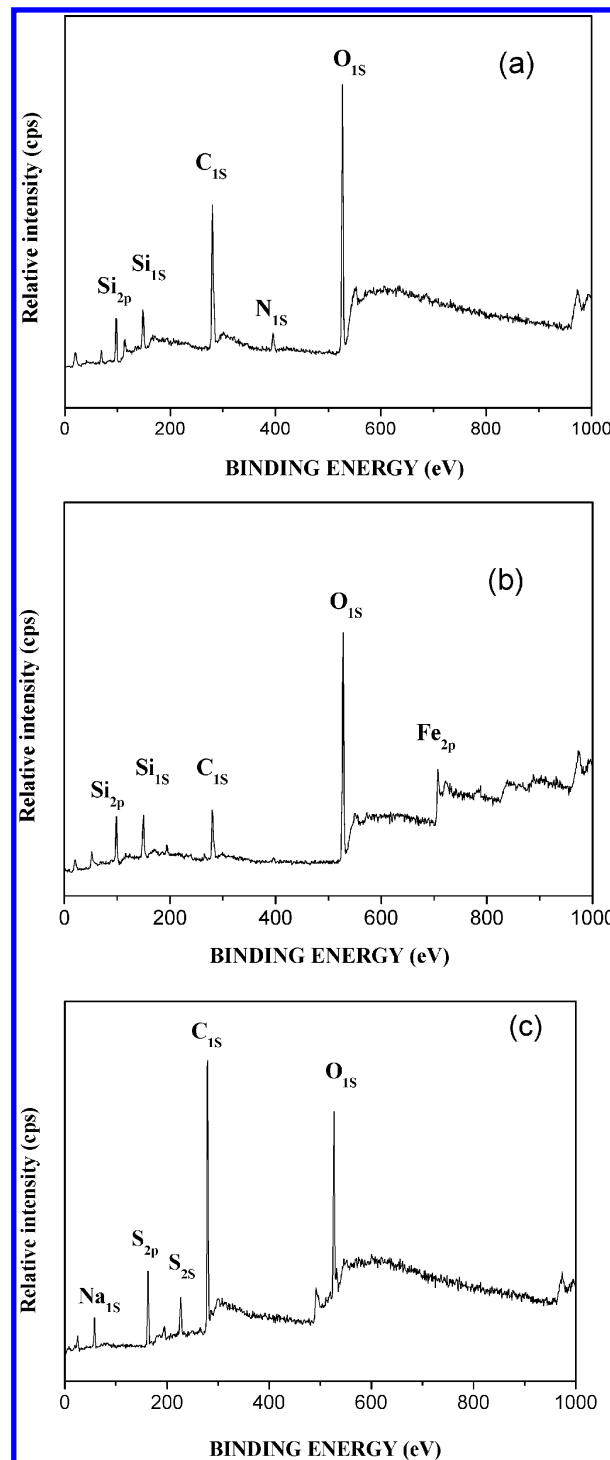


**Figure 3.** XPS survey spectra of (a) a quartz substrate after the acetic acid plasma treatment, (b) the iron-colloid-particle adsorbed substrate, and (c) the PSS adsorbed substrate.

of cationic and anionic components within each of the constituent layers. In addition, the LBL-deposited polymer thin films could form carbon coatings surrounding the intercalated catalyst nanoparticles after calcination to further prevent them from segregation. As a result, therefore, densely packed catalyst particles with a nanometer size could be prepared. Here, we report the use of the layer-by-layer assembling method for the formation of catalyst particles with a controllable size distribution and packing density for synthesizing aligned MWNTs of a controlled structure and morphology.

(27) Liu, Y. J.; Wang, A. B.; Claus, R. O. *Appl. Phys. Lett.* **1997**, *71*, 2265.

(28) Caruso, F.; Spasova, M.; Susha, A.; Giersig, M.; Caruso, R. A. *Chem. Mater.* **2001**, *13*, 109.

(29) Ma, R. Z.; Sasaki, T.; Bando, Y. *J. Am. Chem. Soc.* **2004**, *126*, 10382.

(30) Ago, H.; Komatsu, T.; Ohshima, S.; Kuriki, Y.; Yumura, M. *Appl. Phys. Lett.* **2000**, *77*, 79.

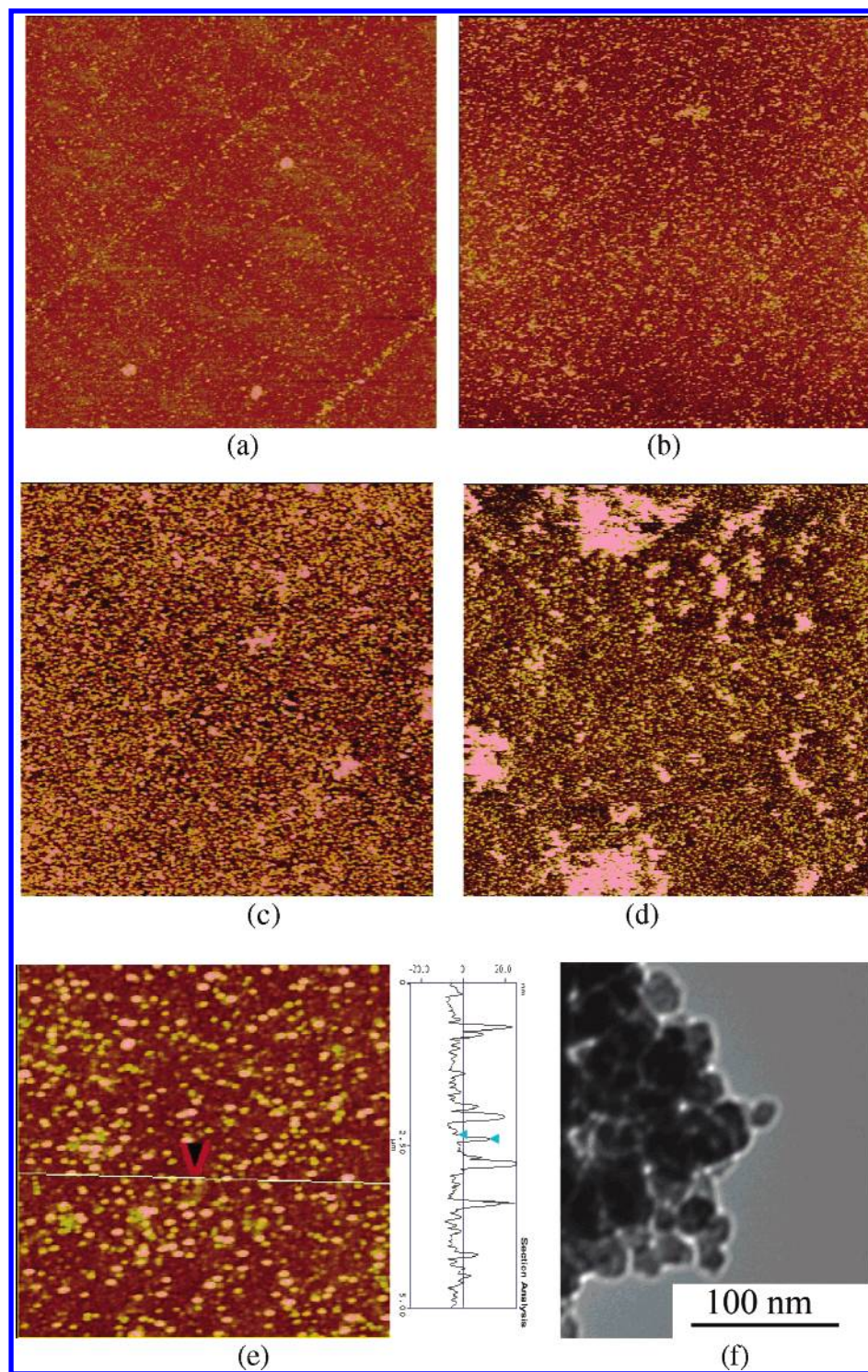


**Figure 4.** AFM images (scanning area =  $20 \times 20 \mu\text{m}^2$ ) of different layer pairs deposited on the quartz substrates after the calcination at  $750^\circ\text{C}$  in  $\text{Ar}/\text{H}_2$  for 5 min: (a, b, c, d) results for 1, 2, 3, and 5 layer pairs, respectively; (e) *left*, as for part b under a higher magnification (scanning area =  $5 \times 5 \mu\text{m}^2$ ), and *right*, line scanning along the path indicated in the left image (height scale =  $-20$  to  $20$  nm); and (f) TEM image for a nanoparticle sample corresponding to part e.

### Experimental Section

**Materials.** Poly(sodium-4-styrenesulfonate), PSS, with a weight-average molecular weight of  $70\,000 \text{ g mol}^{-1}$  and  $\text{FeCl}_3 \cdot 6\text{H}_2\text{O}$  were purchased from Aldrich. A solution of iron hydroxide colloidal particles was prepared by pouring a freshly prepared aqueous solution of  $\text{FeCl}_3$  (0.1 M, 10 mL) into boiling water (90 mL), followed by cooling with air to room temperature. The colloidal particles thus formed were positively charged by the adsorbed positive ions.<sup>31</sup>

**Layer-by-Layer Assembling.** Prior to layer-by-layer self-assembling, the quartz plate was cleaned by immersing it in a bath of concentrated  $\text{H}_2\text{SO}_4$  for 30 min and then thoroughly washing it with double distilled water. This was followed by acetic acid plasma treatment in a custom-built reactor<sup>32</sup> powered by a commercial radio frequency generator at 250

(31) Silva, R. N. *Rev. Pure Appl. Chem.* **1972**, *22*, 115.

(32) Dai, L.; Griesser, H. J.; Mau, A. W. H. *J. Phys. Chem. B* **1997**, *101*, 9548.

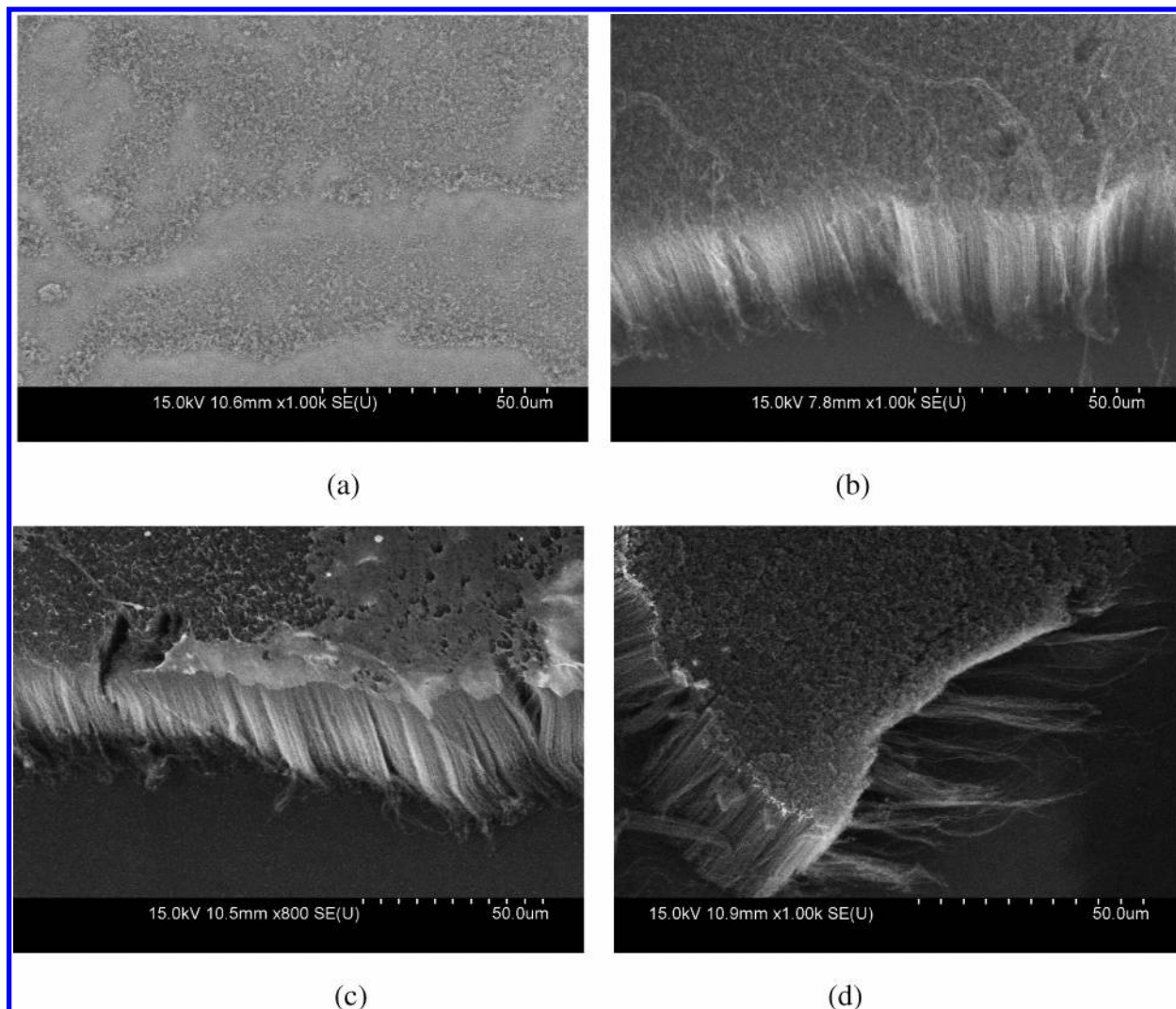


**Figure 5.** SEM images of the carbon nanotubes grown from the  $(\text{PSS}/\text{iron hydroxide colloid particles})_n$  catalyst precursor films of different layer pairs (i.e., different  $n$ ) after the calcination: (a, b, c, d) results for 1, 2, 3, and 5 layer pairs, respectively.

kHz, 30 W, and a monomer pressure of 100 mTorr for 30 s to produce a negatively charged surface (i.e.,  $-\text{COO}^-$ ). Adsorption of the first layer of the iron colloidal nanoparticles was then carried out by immersing the plasma-treated quartz plate in the iron hydroxide colloid solution for 20 min. After washing with double distilled water and drying under ambient atmosphere, the iron-nanoparticle-covered quartz substrate was subsequently used for counterion adsorption in an aqueous solution of PSS ( $1 \text{ mg}\cdot\text{mL}^{-1}$ ). Multilayer films consisting of alternating PSS and iron hydroxide colloid layers,  $(\text{PSS}/\text{iron hydroxide colloid particles})_n$ , were prepared by repeating the above steps for  $n$  times. Figure 1 shows the steps of the layer-by-layer assembling of the iron hydroxide colloidal nanoparticles and PSS, followed by the  $\text{Ar}/\text{H}_2$  reduction of catalyst nanoparticles and the growth of aligned carbon nanotubes.

**Synthesis of Carbon Nanotubes.** The layer-by-layer assembled substrate was heated in  $\text{Ar}/\text{H}_2$  at  $750^\circ\text{C}$  for 5 min (calcination), followed by chemical vapor deposition (CVD) growth of carbon nanotubes on the substrate in a quartz tube furnace under a combined flow of  $\text{Ar}$  (600 sccm),  $\text{H}_2$  (20 sccm), and  $\text{C}_2\text{H}_2$  (20 sccm) at  $750^\circ\text{C}$  for 10 min.

**Characterization.** UV-vis absorption spectra were recorded on an HP-8453 spectrometer, while X-ray photoelec-

tron spectroscopic measurements were made on a VG Microtech ESCA 2000 using monochromatic  $\text{Mg K}\alpha$  radiation at a power of 300 W. Atomic force microscopic (AFM) images were acquired in tapping-mode using a silicon cantilever on a Dimension 3100 AFM with a Nanoscope 5 controller. Scanning electron microscopic (SEM) imaging was performed on a Hitachi S-4800 field emission microscopy. High-resolution transmission electron microscopic (HRTEM) images were taken on a Hitachi H-7600 transmission electron microscope using an accelerating voltage of 120 kV.

## Results and Discussion

**Layer-by-Layer Assembling.** To monitor the layer-by-layer assembling process, we first used a UV-vis spectrometer to measure the increase in optical absorption with increasing layer numbers. Figure 2 shows a typical change of the UV-vis absorption for  $(\text{PSS}/\text{iron hydroxide colloid particles})_n$  multilayer films deposited on the acetic-acid-plasma treated quartz substrate. As can be seen, the increase in absorbance is almost directly proportional to the number of the  $(\text{PSS}/\text{iron hydroxide colloid particles})_n$  layer pairs. The inset plot depicts the absorption intensity at 225 nm vs the number of layer pairs. The linear dependence shown in the inset of Figure 2 clearly indicates the stepwise formation of

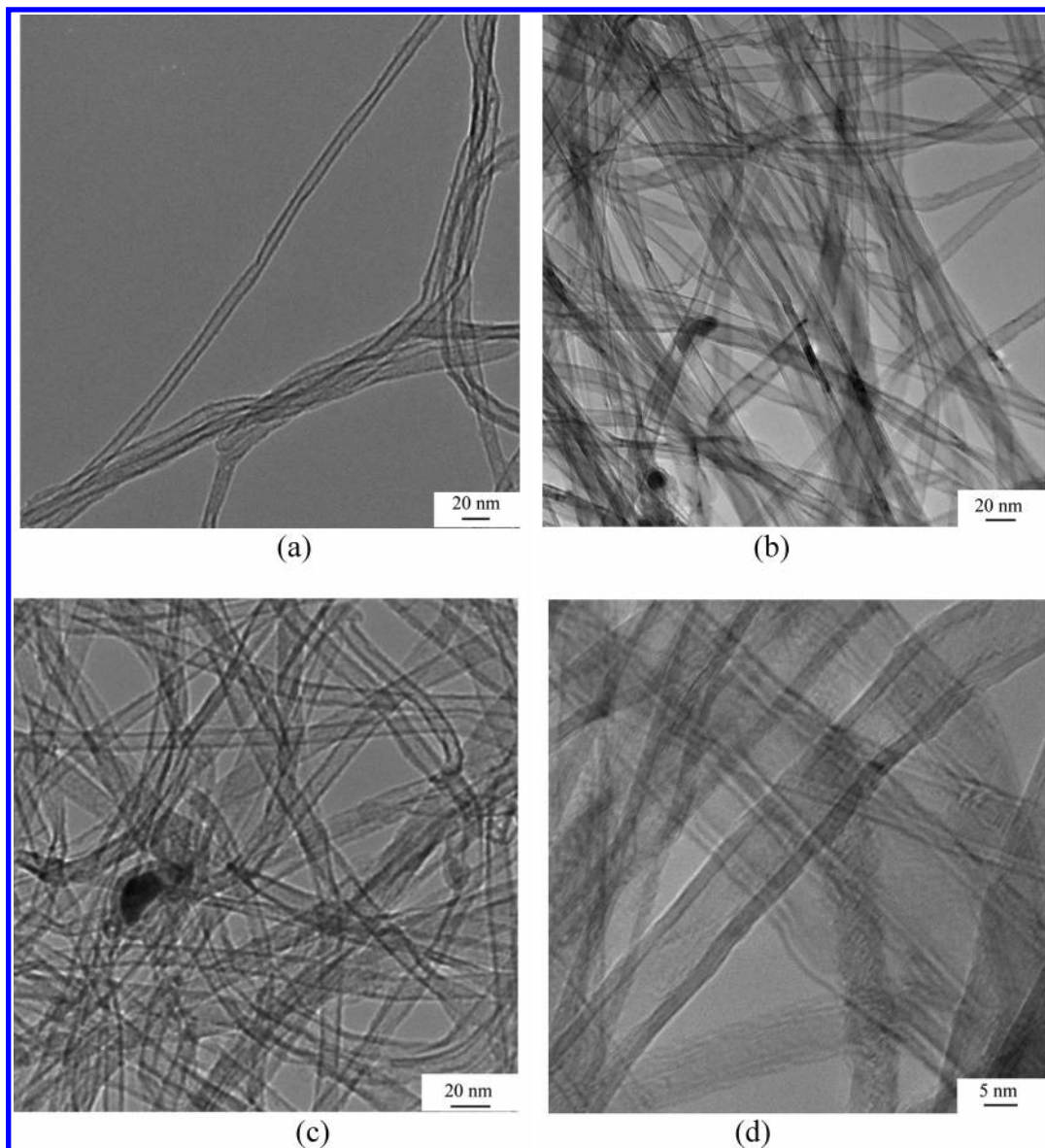


**Figure 6.** TEM images of aligned carbon nanotubes grown from the (PSS/iron hydroxide colloid particles)<sub>n</sub> catalyst precursor films of different layer pairs (i.e., different *n*) after calcination, showing an increase in the nanotube diameter with *n*: (a, b, c) results for *n* = 1, 2, and 5, respectively, and (d) a higher magnification TEM image for the aligned carbon nanotubes corresponding to *n* = 2.

a multilayer film with an approximately equal amount of PSS chains and iron nanoparticles being deposited within each of the constituent layer pairs.<sup>27,29</sup>

Further details for the consecutive formation of the (PSS/iron hydroxide colloid particles) layer pair come from X-ray photoelectron spectroscopic (XPS) studies. Figure 3a shows the XPS survey spectrum of the quartz plate after the plasma treatment. As can be seen, Figure 3a shows a C 1s peak at 285 eV and an O 1s peak at 531 eV, along with the appearance of the Si 2p (106 eV), Si 1s (154 eV), and a weak signal for N 1s (399 eV). The appearance of Si signals from the underlying quartz substrate in Figure 3a indicates that the acetic acid plasma layer is thinner than the XPS probe depth (i.e., 10 nm)<sup>33</sup> due to a short plasma-deposition time (30 s). The N 1s peak can be attributed to adsorbed gaseous molecules from the air. Figure 3b reproduces the XPS survey spectrum of the iron-colloid-particle adsorbed substrate,

which clearly shows the Fe 2p peak at 708 eV along with signals for C 1s (285 eV), O 1s (531 eV), Si 2p (106 eV), and Si 1s (154 eV) from the underlying plasma/quartz layers. The removal of the adsorbed nitrogen molecules during the iron hydroxide deposition process is evident by the loss of the N 1s signal in Figure 3b. The significant increase in the O/C atomic ratio from part a to part b of Figure 3 is consistent with the effective deposition of iron hydroxide particles.

As expected, XPS measurements on the PSS adsorbed substrate reveal new peaks at 227, 164, and 60 eV attributable to S 2s, S 2p, and Na 2s, respectively. The disappearance of Si and Fe signals in Figure 3c indicates that the newly formed PSS layer is pinhole-free and thicker than the XPS probe depth (i.e., > 10 nm). Therefore, the XPS results unambiguously indicate that both the iron hydroxide colloid particles and the PSS chains have been alternatively assembled onto the acetic-acid-plasma treated quartz surface during the layer-by-layer assembling process.

(33) *Methods of Surface Analysis: Techniques and Applications*; Walls, J. M., Ed.; Cambridge University Press: Cambridge, U.K., 1990.

**Catalyst Particle Formation.** Figure 4 shows AFM images for the multilayer films of (PSS/iron colloidal particles)<sub>n</sub> with different *n* after calcination. As can be seen, the surface packing density of the iron nanoparticles increased rapidly with increasing *n* (Figure 4 parts a–d). The increase in the particle packing density with the deposition cycles was accompanied by a gradual increase in the particle size (Figure 4 parts a–d). While the rapid increase in the particle packing density with the deposition cycles indicates a steady introduction of the Fe catalyst component at each of the deposition steps, the relatively slow concomitant increase in the particle size suggests that the LBL-deposited polymer thin films have effectively prevented the catalyst nanoparticles from segregation during the calcination process. The enlarged AFM image given in Figure 4e for Figure 4b clearly shows uniformly distributed nanoparticles of an average diameter of ca. 15 nm were produced after calcination of a (PSS/iron hydroxide colloidal particles)<sub>2</sub> multilayer film on the quartz substrate in Ar/H<sub>2</sub> at 750 °C for 5 min. The corresponding TEM image in Figure 4f indeed shows the presence of a thin carbon protective coating around the catalyst particles. Therefore, the layer-by-layer assembling should, in principle, enable us to prepare uniformly dispersed catalyst nanoparticles with a controllable packing density and size distribution by simply regulating the number of deposition cycles and/or relative amounts of the cationic and anionic components within each of the constituent layers.

**Aligned Carbon Nanotube Growth.** Following previous work on the growth of aligned MWNTs from iron nanoparticles reported by several groups,<sup>10–15</sup> including us,<sup>10</sup> we proceeded to use the layer-by-layer assembled iron catalyst nanoparticles on the quartz plate for *controlled* synthesis of aligned carbon nanotubes by pyrolysis of acetylene under a combined flow of Ar (600 sccm) and H<sub>2</sub> (20 sccm) at 750 °C for 10 min.

Figure 5 shows SEM images taken from carbon nanotubes grown from the iron catalyst nanoparticles produced with different numbers of the layer pairs. As can be seen in Figure 5a, nonaligned carbon nanotubes were formed on the quartz plate with one layer pair due, most probably, to a low surface density of the iron catalyst nanoparticles on this particular substrate surface (cf. Figure 4a). Partially aligned carbon nanotubes (Figure 5b), however, were prepared from the (PSS/iron hydroxide colloid particles)<sub>n</sub> catalyst precursor films with two layer pairs (i.e., *n* = 2). Further increasing the number of the (PSS/iron colloidal particles) layer pairs led to the formation of well-aligned carbon nanotubes with a uniform length of about 25 micrometer (parts c and d of Figure 5). It can also be seen in Figure 5 that the packing density of the resultant aligned carbon nanotubes increased with increasing *n*. Comparing Figure 5 with Figure 4 indicates, once again, that densely packed catalyst nanoparticles are necessary for the aligned growth of carbon nanotubes and that the aligned carbon nanotubes grown on the substrate with a higher *n* value possess a more straight structure, because a high surface packing density of the growing carbon nanotubes can ensure the constituent nanotubes are “uncoiled” during the growth process.<sup>34</sup>

TEM examinations revealed that the outer diameter of the resultant carbon nanotubes increased with increasing number of the (PSS/iron colloidal particles) layer pairs (Figures 6

parts a–c). In addition, the higher-magnification TEM image of carbon nanotubes (Figure 6d) taken from an aligned nanotube array produced on a (PSS/iron colloidal particles)<sub>2</sub> catalyst precursor film shows a reasonably graphitized structure with an outer diameter of ca. 15 nm, consistent with the nanoparticle size (cf. Figure 4e). The above results indicate that there is considerable room for regulating packing density and size distribution of the catalyst nanoparticles, and hence the morphology and structure of carbon nanotubes subsequently formed, by simply changing the deposition cycle numbers during the layer-by-layer assembling process. Therefore, aligned carbon nanotubes with a controlled structure and morphology can be readily produced by judiciously designing the layer-by-layer assembling process.

## Conclusions

We have demonstrated that the layer-by-layer assembling process can be applied to fabricate catalyst particles of a controllable size distribution and packing density on appropriate substrates for controlled synthesis of aligned carbon nanotubes with a specific structure and morphology. In particular, we have prepared poly(sodium-4-styrenesulfonate) and iron hydroxide colloid multilayer films via the layer-by-layer assembling onto an acetic-acid-plasma treated quartz plate, followed by reducing with Ar/H<sub>2</sub> at 750 °C (i.e., calcination) and subsequent carbon nanotube growth by pyrolysis of acetylene in a quartz tube furnace under a combined flow of Ar and H<sub>2</sub> at 750 °C. UV–vis absorption and XPS spectroscopic measurements, together with AFM imaging, confirm the consecutive formation of iron hydroxide colloidal particles/PSS multilayer catalyst precursor films. The layer-by-layer assembling was shown to possess advantages in not only providing an easy control of the particle packing density and size distribution by simply regulating the layer number but also allowing the layered polymer thin films to form thin carbon coatings surrounding the intercalated catalyst nanoparticles to prevent them from segregation during the calcination and nanotube growth processes. SEM and TEM images show the formation of perpendicularly aligned carbon nanotubes with a layer-number-dependent tube diameter and packing density. Aligned carbon nanotubes with a controlled structure and morphology were produced by simply controlling the layer number. The highly generic nature of the layer-by-layer assembling,<sup>25,26</sup> together with the ease with which colloidal solutions can be prepared from a large variety of metal ions, could make the methodology developed in this study a general and effective approach toward the controlled synthesis of aligned carbon nanotubes for many potential applications.

**Acknowledgment.** The authors thank the NSF (CCF-0403130), ACS (PRF 39060-AC5M), AFOSR, AFRL/ML, Wright Brothers Institute, Dayton Development Collaborations, Honda, and University of Dayton for financial support. We gratefully acknowledge the assistance by Drs. Liangti Qu, Wei Chen, Thomas Wittberg, and Kyung Min Lee and the NEST Lab at UD for the access of SEM and TEM facilities.

CM051512L